Reversible Interaction of β-Actin Along the Channel of the TCP-1 Cytoplasmic Chaperonin

S. Marco, J. L. Carrascosa, and J. M. Valpuesta
Centro Nacional de Biotecnología, C.S.I.C., Campus Universidad Autónoma, Cantoblanco, 28049 Madrid, Spain

ABSTRACT The cytoplasm of eukaryotes contains a heteromeric toroidal chaperonin assembled from the t-complex TCP-1 and several other related polypeptides. The structure of the TCP-1 cytoplasmic chaperonin and that of the binary complex formed between this chaperonin and unfolded β-actin have been studied using electron microscopy and image processing techniques. Two-dimensional averaging of front views reveals a circular stain-excluding mass surrounding a central stain-penetrating region in which the stain is excluded upon actin binding. Sections of a three-dimensional reconstruction of the chaperonin show that the inner core is an empty channel that becomes filled upon binary complex formation with unfolded β-actin. Upon incubation with Mg-ATP, the β-actin:chaperonin complex discharges the actin such that the chaperonin central cavity reappears. Side views from different forms of TCP-1 reveals that upon Mg-ATP binding, the cytoplasmic chaperonin undergoes a structural rearrangement that is confirmed using a new classification method.

INTRODUCTION

Chaperones are a family of proteins or protein complexes that are involved in promoting the correct folding or assembly of polypeptides (Hemmingsen et al., 1988, Bockhareva et al., 1988, Cheng et al., 1989; Ellis and van der Vies, 1991). The best known members of this family are the chaperonins, composed of proteins with a molecular weight close to 60 kDa which, in common with other chaperones, inhibit the improper folding of a large number of proteins (Zeilstra-Ryalls et al., 1991; Gething and Sambrook, 1992; Hartl and Martin, 1992). Their structure has been studied at low resolution by electron microscopy and is generally composed of two stacked rings. Chaperonins have been classified into two groups: one contains those chaperonins of bacterial origin like GroEL (Hendrix, 1979; Hohn et al., 1979) or from eukaryotic organelles (such as the mitochondrial Hsp60 (Viitanen et al., 1992) or the Rubisco binding protein from chloroplasts (Barraclough and Ellis, 1980)). The second group contains chaperonins from thermophilic bacteria such as TF55 from *Sulfolobus shibatae* (Trent et al., 1991) or *S. solfataricus* (Marco et al., 1994), and the eukaryotic cytosolic TCP-1 (Ursic and Culberston, 1991; Gao et al., 1992; Yaffe et al., 1992; Lewis et al., 1992; Frydman et al., 1992).

The heteromeric cytoplasmic chaperonin TCP-1 (chaperonin or cytoplasmic chaperonin) is assembled from t-complex polypeptide 1 (TCP-1), which is homologous to TF55 from *S. shibatae* (Trent et al., 1991), and also from other homologous polypeptides with a molecular mass ranging from 55 to 62 kDa (Gao et al., 1992; Yaffe et al., 1992; Lewis et al., 1992; Frydman et al., 1992). This chaperonin has been found to promote the in vitro folding of β-actin (Gao et al., 1992) and α- and β-tubulin (Yaffe et al., 1992; Gao et al., 1993), although in the last case two additional factors are also needed (Gao et al., 1993). It has recently been reported that the cytoplasmic chaperonin is capable of promoting the folding of actin and tubulin in vivo (Sternlicht et al., 1993). The TCP-1 chaperonin is not restricted to the cytosol of mammalian cells, since an homologous complex has been isolated from etiolated oat seedlings (Mummert et al., 1993). The molecular aggregate formed by this protein is capable of stimulating the refolding of denatured phytochrome to a photoactive form in the presence of Mg-ATP. However, in spite of the amino acid sequence similarity between the t-complex polypeptide 1 and this protein, the morphology (as seen by electron microscopy) of the aggregates assembled from each of these proteins is very different (Gao et al., 1992; Lewis et al., 1992; Mummert et al., 1993). In this work, we report a comparison of the two-dimensional images of the cytoplasmic chaperonin and the complex formed by this chaperonin with the unfolded β-actin, together with changes in the quaternary structure promoted by Mg-ATP binding. These changes are confirmed by use of a newly devised classification method that has proved useful in separating populations containing slight structural differences.

MATERIALS AND METHODS

Specimen preparation

Uncomplexed chaperonin and β-actin:chaperonin complex, a kind gift of Dr. N. Cowan, were prepared from rabbit reticulocyte lysate as described by Gao et al. (1992). Actin was released from the binary complexes by incubation with 10 mM $MgCl_2$ and 10 mM ATP for 1 h at 30°C in 20 mM MES, pH 6.9, 0.1 M KCl, 1 mM EGTA, 1 mM dithiothreitol. When needed, uncomplexed chaperonin was also incubated with 10 mM Mg-ATP in the same buffer.

Electron microscopy and image processing

Aliquots of the samples were applied to carbon-coated collodion grids and stained with 1% uranyl acetate. Images were recorded on Kodak film SO-163 using a JEOL 1200EX-II electron microscope operated at 100 kV with

Received for publication 9 February 1994 and in final form 27 April 1994.

Address reprint requests to J. M. Valpuesta, Centro Nacional de Biotecnología, Universidad Autónoma de Madrid, 28049 Madrid, Spain. Tel.: 34 1 5854550; Fax: 34 1 5854506; E-mail: jmv@samba.cnb.uam.es.

0006-3495/94/07/364/05 $2.00

a low-dose kit. Micrographs were recorded at 0° and at a magnification of 50,000×. Micrographs were digitized using a Eikonix IEEE-488 camera with a sampling window corresponding to 4.7 Å/pixel. Image processing of individual particles was carried out as described by Carrascosa et al. (1990), except that average images were calculated using an improved alignment algorithm (Penczek et al., 1992; Marco et al., 1993). In the case of actin binary complex preparations, particles having a central stain-filled domain were separated from those showing a stain-penetrating central region using a Kohonen-based self-organizing map classifier (Kohonen, 1990; Marabini and Carazo, 1994). The number of output code vectors was 25 and they were placed following a hexagonal topology. The rest of the parameters were the same as those used in Marabini and Carazo (1994). The same method was used in the classification of side views. The resolution was calculated using the spectral signal-to-noise ratio method (Unser et al., 1987). Three-dimensional reconstructions were carried out from micrographs of negatively stained uncomplexed chaperonin and β-actin:chaperonin complex recorded at 55° and 0°, at a magnification of 50,000×, using the random conical tilt series method (Radermacher et al., 1987).

RESULTS AND DISCUSSION

When negatively stained chaperonin particles were observed in the electron microscope (Fig. 1 *A*), two types of structure were clearly seen: a doughnut-shaped particle (Trent et al., 1991) and a less common barrel-shaped structure (Phipps et al., 1993), with two prominent striations across the central portion. Because of their similarity to front and side views of the *Escherichia coli* chaperonin GroEL, we call these images front and side views, respectively, of this chaperonin. When front and side views were independently averaged using the alignment procedure described in Materials and Methods, their characteristic features, similar to those found in the chaperonins from archaebacteria (Trent et al., 1991; Phipps et al., 1993), were more clearly evident. The average front view obtained after processing 394 particles (Fig. 2 *A*) reveals a stain-filled region in the center surrounded by a complex stain-excluding layer. The diameter of the particle is around 16 nm, while that of the channel is around 6 nm. The mass is distributed radially showing the presence of 8 slightly asymmetrical mass units. This result contrasts with

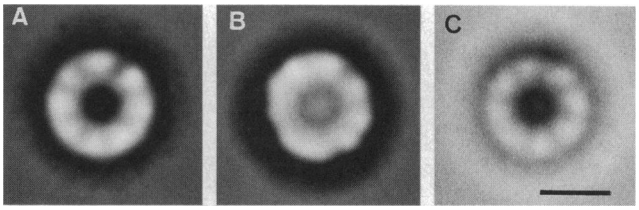

FIGURE 2 Average image of front views of uncomplexed cytoplasmic chaperonin (*A*), actin:chaperonin complex (*B*), and chaperonin (*C*) after the release of bound actin by incubation with Mg-ATP. Scale bar = 10 nm.

the symmetrical distribution of the mass units in the average image obtained for the related thermophilic chaperonin from *Pyrodictium occultum* (Phipps et al., 1993), probably because of the higher complexity of the cytoplasmic chaperonin (Rommelaere et al., 1993). The average side view obtained after processing 393 particles (Fig. 4, *A* and *C*) shows the barrel-shaped structure described above, with dimension of 15 × 16 nm and four parallel striations that, unlike those of *P. occultum* (Phipps et al., 1993) and *P. brockii* (Phipps et al., 1991), are very similar in thickness.

A three-dimensional reconstruction carried out from 193 negatively stained particles using the random conical tilt series method (Radermacher et al., 1987) (Fig. 3 *A*) confirmed the presence of a channel that is open throughout the particle. The dimensions of the average side and front views and the non-rectangular side view suggest a model in which the cytoplasmic chaperonin is composed of two rings juxtaposed face-to-face, in a similar way to the stacking of the paired rings in GroEL (Langer et al., 1992).

It has been shown that the cytoplasmic chaperonin forms a stable binary complex with denatured actin (Gao et al., 1992). To locate the actin binding site within the chaperonin particle, β-actin:chaperonin complexes were prepared and observed in the electron microscope (Fig. 1 *B*). In these preparations, two different populations could be distinguished: the first (50% of the total population) showed the

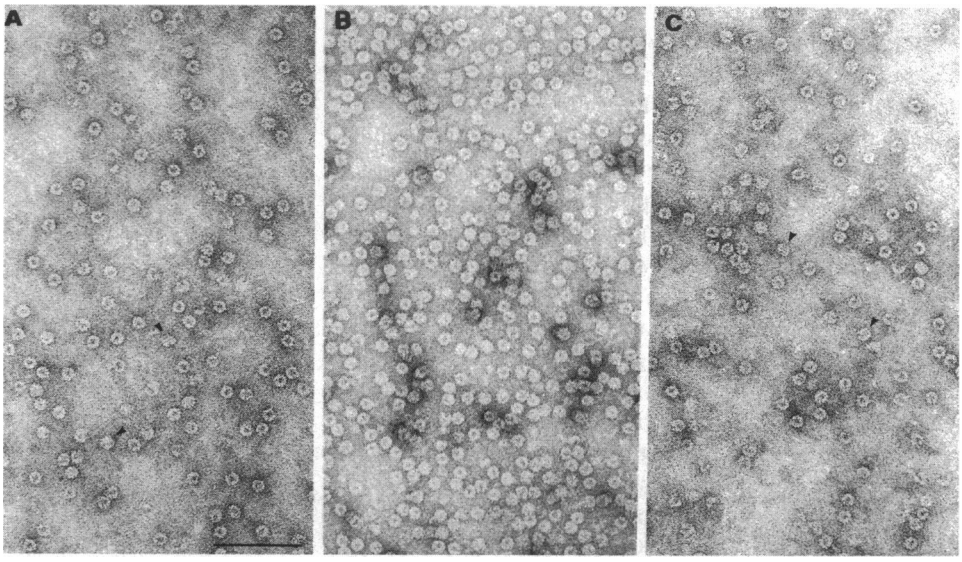

FIGURE 1 Electron micrographs of uncomplexed chaperonins (*A*), actin:chaperonin complexes (*B*), and chaperonins (*C*) after the release of bound actin. Most of the particles are front views, but side views can also be seen in *A* and *C* (*arrows*). Scale bar = 100 nm.

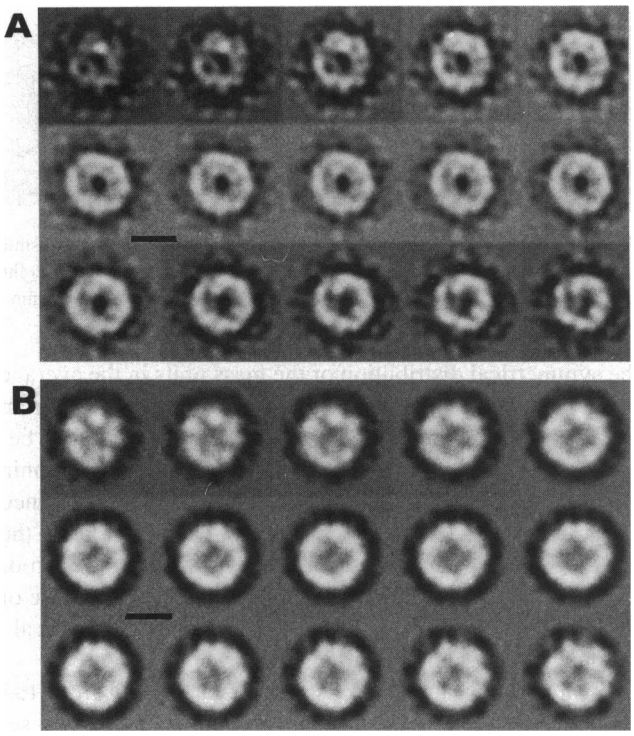

FIGURE 3 Sections through the three-dimensional reconstruction of uncomplexed cytoplasmic chaperonin (3.6 nm resolution) (*A*) and actin:chaperonin complex (4.2 nm resolution) (*B*). Distance between successive sections is 0.47 nm. Scale bar = 10 nm.

stain-filled central region observed in front views of uncomplexed cytoplasmic chaperonin, whereas the second lacked the stain-filled central domain. This probably reflects a heterogeneous population consisting of uncomplexed chaperonins and β-actin:chaperonin complexes generated when unfolded β-actin is presented to chaperonin in the absence of Mg-ATP. When the two populations were separated using the newly devised Kohonen-based classifier (Marabini and Carazo, 1994) and 437 of the particles lacking the stain-filled central domain were processed, the average view obtained (Fig. 2 *B*) revealed that the channel is filled with a stain-excluding mass, specially in the center of the channel, reminiscent of the images of complexes formed between alcohol oxidase or rhodanese and GroEL or GroEL-GroES complexes (Langer et al., 1992). Recently, experiments carried out with dihydrofolate reductase (DHFR):GroEL complexes in which the unfolded DHFR was labeled with 1.4 nm gold clusters, located the unfolded protein in the front portions of the channel (Braig et al., 1993). This result is consistent with a three-dimensional reconstruction carried out with β-actin:chaperonin complexes (188 particles), which shows that sections of the three-dimensional map contain a stain-excluding mass all along the channel (Fig. 3 *B*). The low resolution of this reconstruction (4.2 nm), especially in the direction perpendicular to the plane of the rings, makes the area occupied by the unfolded actin larger than it probably is, thus preventing an accurate location of the folding peptide.

When β-actin:chaperonin complexes were incubated with Mg-ATP, actin was released (Gao et al., 1992) and the particles observed by electron microscopy revealed the typical front and side views (Fig. 1 *C*), with the front views clearly showing the stain-filled region in the center of the particle. The average image of front views after processing of 361 particles (Fig. 2 *C*) is very similar to the uncomplexed chaperonin views (Fig. 2 *A*) and confirms the presence of the empty channel that reappears upon release of the folded actin. These results reinforce the notion that the central cavity is the binding site of unfolded actin within the cytoplasmic chaperonin, and that the particle returns to its original structure after actin liberation.

The effect of binding of ATP (in the presence of magnesium) on the structure of the cytoplasmic chaperonin has also been studied. The average side view obtained from 452 images of the chaperonin incubated in the presence of Mg-ATP showed some different features from that obtained from 393 particles of the uncomplexed chaperonin (Fig. 4). The overall structure of the chaperonin shows a a barrel-shaped outline (Fig. 4, *A* and *C*), while after incubation with Mg-ATP the projection profile changes toward something compatible with two truncated cones (Fig. 4, *B* and *D*). Together with this change in the profile, the stain-filled cavities also appear

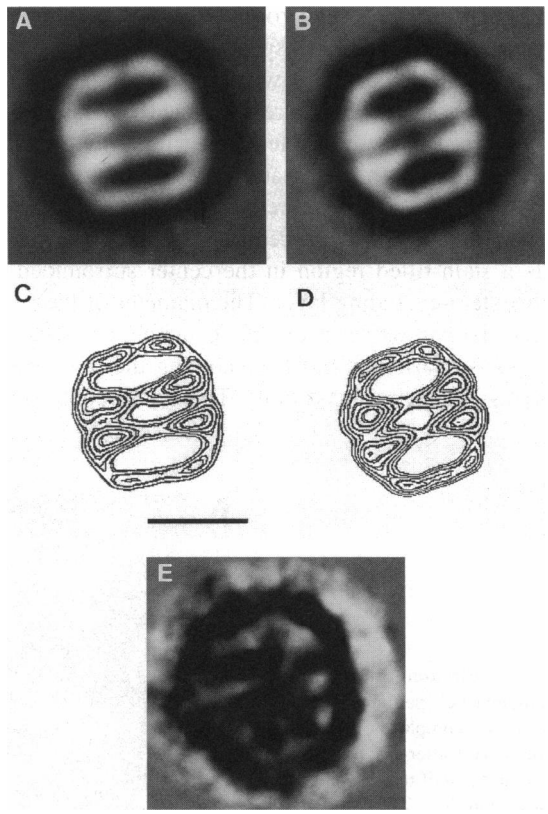

FIGURE 4 Average image of side views of uncomplexed cytoplasmic chaperonin (*A*) and chaperonin incubated with Mg-ATP (*B*). (*C*) and (*D*): corresponding gray-level images of *A* and *B*. (*E*): difference map obtained after dividing the difference between the average images *A* and *B* by the standard error of the difference (obtained from the variance within each average). Student's *t*-test (Brandt, 1970) was used to assess the significance of the differences, with $t_{max} = 14.5$ and $t_{min} = -26.9$, showing that the differences are highly significant. Scale bar = 10 nm.

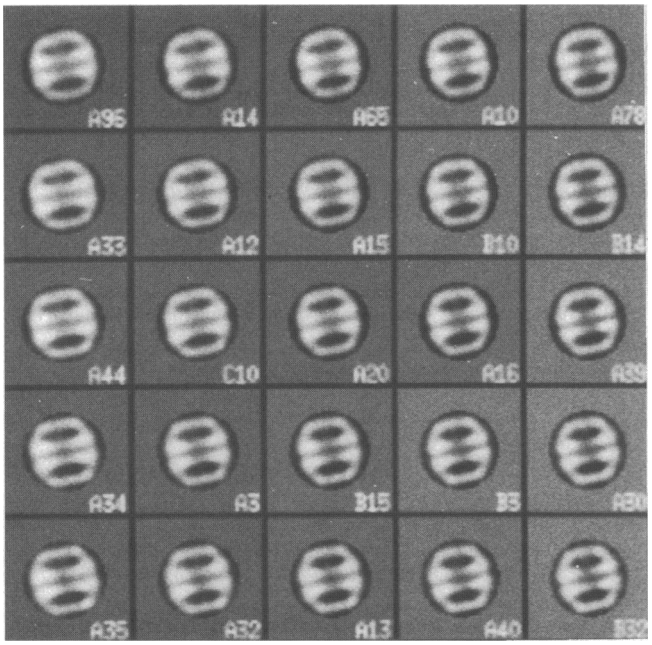

FIGURE 5 Dictionary output vectors corresponding to a Kohonen-based image classification of a mixed population of chaperonins incubated with or without Mg-ATP. The number shown at the bottom right of the code vector images corresponds to the number of particles represented by each vector.

different, probably as a consequence of the rearrangement generated in each of the two rings that is reflected in a different relative orientation of the longitudinal and transverse domains. Several methods were used to check whether the averages were from different populations and not due to sample fluctuations from the same population. A significant difference map was obtained (Fig. 4 *E*) after dividing the difference between the average images from the uncomplexed chaperonin (Fig. 4 *A*) and the chaperonin incubated with Mg-ATP (Fig. 4 *B*) by the standard error of the difference (obtained from the variance within each average). A similar result is obtained after quantitative substraction of both average images, following a substraction algorithm devised by Carrascosa and Steven (1978) (results not shown). Although these differences were found to be significant for different sample batches and processing experiments, a different method was also used to make a more objective assessment of each population. Populations incubated with Mg-ATP (represented by the average image of Fig. 4 *B*) or without Mg-ATP (represented by the average image of Fig. 4 *A*) were mixed and subjected to a Kohonen-based self-organizing map. Fig. 5 shows a dictionary of output vectors after the classification, in which most of the Mg-ATP bound chaperonins have been placed in the bottom right vectors and those not incubated with ATP in the top left vectors. Central vectors show the particles of both populations that could not be classified. This result clearly indicates that the Mg-ATP bound chaperonins can be separated from those that have not been incubated with Mg-ATP using appropriate classification techniques and points to a significant structural difference between each population. This is confirmed by the fact that when Mg-ATP bound chaperonin was incubated in the presence of excess ADP and side views of this sample were processed, the average image obtained shows similar features to those found in the original uncomplexed particles (data not shown). Structural differences induced in chaperonins upon Mg-ATP binding have already been described for the chaperonin from *Rhodobacter sphaeroides* (Saibil and Wood, 1993) and suggest that upon Mg-ATP binding, the cytoplasmic chaperonin undergoes a large structural rearrangement that is reflected in the shape of each of the toroids and in the way both interact. The hypothesis of a structural rearrangement generated by the presence of Mg-ATP is reinforced by the finding that the average image of side views of β-actin:chaperonin complexes incubated with Mg-ATP clearly resembles that of the chaperonin not incubated with Mg-ATP (data not shown). In this case, although the actin: chaperonin complexes have been incubated with ATP, this is rapidly hydrolyzed to release the folded substrate (Gao et al., 1992; Yaffe et al., 1992).

Studies at higher resolution will be needed to further understand the nature of the interactions between the chaperonin and the unfolded polypeptide. Nonetheless, our data clearly define the central core of the cytoplasmic chaperonin as the domain where facilitated folding takes place and reveal a conformational change in the quaternary structure of the two rings of the cytoplasmic chaperonin upon interaction with ATP.

We thank Dr. N. J. Cowan for the kind gift of samples of TCP-1 chaperonin and the β-actin:chaperonin complex. We thank Dr. J. M. Carazo and R. Marabini for allowing us the use of their unpublished classification methods and their careful reading of the manuscript.

This work was partly supported by Grant PB91–0109 from the Dirección General de Investigación Científica y Técnica. S.M. is a recipient of a fellowship from the Comunidad Autónoma de Madrid.

REFERENCES

Barraclough, R., and R. J., Ellis. 1980. Protein synthesis in chloroplasts. IX. Assembly of newly-synthesized large subunits into ribulose biphosphate carboxylase in isolated intact pea chloroplasts. *Biochim. Biophys. Acta.* 608:19–31.

Bochkareva, E. S., N. M. Lissin, and A. S. Girshovich. 1988. Transient association pf newly synthesized unfolded proteins with the heat-shock GroEL protein. *Nature.* 336:254–257.

Braig, K., M. Simon, F. Furuya, J. F. Hainfeld, and A. L. Horwich. 1993. A polypeptide bound by the chaperonin GroEL is localized within a central cavity. *Proc. Natl. Acad. Sci. USA.* 90:3978–3982.

Brandt, S. 1970. Statistical and Computational Methods in Data Analysis. North-Holland Publishing, Amsterdam.

Carrascosa, J. L., G. Abella, S. Marco., and J. M. Carazo. 1990. Three-dimensional reconstruction of the sevenfolded form of *Bacillus subtilis* GroEL chaperonin. *J. Struct. Biol.* 106:211–220.

Carrascosa, J. L., and A. C. Steven. 1978. A procedure for evaluation of significant structural differences between related arrays of protein molecules. *Micron.* 9:199–206.

Cheng, M. Y., F. U. Hartl, J. Martin, R. A. Pollock, F. Karlousek, W. Neupert, E. M. Hallberg, R. L. Hallberg, and A. L. Horwich. 1989. Mitochondrial heat-shock protein hsp60 is essential for assembly of proteins imported into yeast mitochondria. *Nature* 337:620–625.

Ellis, R. J., and S. M. Van der Vies. 1991. Molecular chaperones. *Annu. Rev. Biochem.* 60:321–347.

Frydman, J., E. Nimmesgern, H. Erdjument-Bromage, J. S. Wall, P. Tempst, and F. U. Hartl. 1992. Function in protein folding of TRiC, a cytosolic ring complex containing TCP-1 and structurally related subunits. *EMBO J.* 11:4767–4778.

Gao, Y., J. O. Thomas, R. L. Chow, G. H. Lee., and N. J. Cowan. 1992. A cytoplasmic chaperonin that catalyzes β-actin folding. *Cell.* 69: 1043–1050.

Gao, Y., I. E. Vainberg, R. L. Chow, and N. J. Cowan. 1993. Two cofactors and cytoplasmic chaperonin are required for the folding of α- and β-tubulin. *Mol. Cell. Biol.* 13:2478–2485.

Gething, M. J., and J. Sambrook. 1992. Protein folding in the cell. *Nature.* 355:35–45.

Hartl, F. U., and J. Martin. 1992. Protein folding in the cell: the roles of molecular chaperones Hsp70 and Hsp60. *Annu. Rev. Biophys. Biomol. Struct.* 21:293–322.

Hemmingsen, S. M., C. Woolford, S. M. Van der Vies, K. Tilly, D. T. Dennis, C. P. Georgopoulos, R. W. Hendrix, and R. J. Ellis. 1988. Homologous plant and bacterial proteins chaperone oligomeric protein assembly. *Nature.* 333:330–334.

Hendrix, R. W. 1979. Purification and properties of GroE, a host protein involved in bacteriophage assembly. *J. Mol. Biol.* 129:375–392.

Hohn, T., B. Hohn, A. Engel, M. Wurtz, and P. R. Smith. 1979. Isolation and characterization of the host protein GroE involved in bacteriophage lambda assembly. *J. Mol. Biol.* 12:359–373.

Kohonen, T. 1990. The self organizing map. *Proc. IEEE.* 78:1464–1480.

Langer, T., G. Pfeifer, J. Martin, W. Baumeister, and F. U. Hartl. 1992. Chaperonin-mediated protein folding: GroES binds to one end of the GroEL cylinder, which accommodates the protein substrate within its central cavity. *EMBO J.* 11:4757–4765.

Lewis, V. A., G. M. Hynes, D. Zheng, H. Saibil, and K. Willison. 1992. T-complex polypeptide-1 is a subunit of a heteromeric particle in the eukaryotic cytosol. *Nature.* 358:249–252.

Marabini, R., and J. M. Carazo. 1994. Pattern recognition and classification of images of biological macromolecules using artificial neural networks. *Biophys. J.* In press.

Marco, S., D. Ureña, J. L. Carrascosa, T. Waldmann, J. Peters, R. Hegerl, G. Pfeifer, H. Sack-Kongehl, and W. Baumeister. 1994. The molecular chaperone TF55: assessment of symmetry. *FEBS Lett.* 341:152–155.

Marco, S., J. M. Valpuesta, G. Rivas, G. Andrés, C. San Martín, and J. L. Carrascosa. 1993. A structural model for the GroEL chaperonin. *FEMS Microbiol. Lett.* 106:301–308.

Mummert, E., R. Grimm, V. Speth, C. Eckerson, E. Schiltz, A. A. Gatenby, and E. Schäfer. 1993. A TCP1-related molecular chaperone from plants refolds phytochrome to its photoreversible form. *Nature.* 363:644–648.

Penczek, P., M. Radermacher, and J. Frank. 1992. Three-dimensional reconstruction of single particles embedded in ice. *Ultramicroscopy.* 40: 33–53.

Phipps, B. M., A. Hoffmann, K. O. Stetter, and W. Baumeister. 1991. A novel ATPase complex selectively accumulated upon heat shock is a major cellular component of thermophilic archaebacteria. *EMBO J.* 7:1711–1722.

Phipps, B. M., D. Typke, R. Hegerl, S. Volker, A. Hoffmann, K. O. Stetter, and W. Baumeister. 1993. Structure of a molecular chaperone from a thermophilic archaebacterium. *Nature.* 361:475–477.

Radermacher, M. J., T. Wagenknetch, A. Verschoor, and J. Frank. 1987. Three-dimensional reconstruction from a single-exposure random conical tilt series applied to the 50S ribosomal subunit of *Escherichia coli.* *J. Microsc.* 146:113–136.

Rommelaire, H., M. Van Troys, Y. Gao, R. Melki, N. J. Cowan, J. Vandekerchove, and C. Ampe. 1993. Eukaryotic cytosolic chaperonin contains T-complex polypeptide 1 and seven related subunits. *Proc. Natl. Acad. Sci. USA.* 90:11975–11979.

Saibil, H., and S. Wood. 1993. Chaperonins. *Curr. Opin. Struct. Biol.* 3: 207–213.

Sternlicht, H., G. W. Farr, M. L. Sternlitch, J. M. Driscoll, K. Willison, and M. B. Yaffe,. 1993. The T-complex polypeptide 1 complex is a chaperonin for tubulin and actin *in vivo. Proc. Natl. Acad. Sci. USA.* 90: 9422–9426.

Trent, J. D., E. Nimmesgern, J. S. Wall, F. U. Hartl, and A. L. Horwich. 1991. A molecular chaperone from a thermophilic archebacterium is related to the eukaryotic protein T-complex polypeptide 1. *Nature.* 354: 490–493.

Unser, M, B. L. Trus, and A. C. Steven. 1987. A new resolution criterion based on spectral signal-to-noise method ratios. *Ultramicroscopy.* 23: 39–52.

Ursic, D., and M. R. Culberston. 1991. The yeast homologue to mouse Tcp-1 affects microtubule mediated processes. *Mol. Cell. Biol.* 11: 2629–2640.

Viitanen, P. V., G. H. Lorimer, R. Seetharam, R. S. Gupta, J. Oppenheim, J. O. Thomas, and N. J. Cowan. 1992. Mammalian mitochondrial chaperonin 60 functions as a single toroidal ring. *J. Biol. Chem.* 267:695–698.

Yaffe, M. B., G. W. Farr, D. Miklos, A. L. Horwich, M. L. Sternlicht, and H. Sternlicht. 1992. TCP1 complex is a molecular chaperone in tubulin biogenesis. *Nature.* 358:245–248.

Zeilstra-Ryalls, J., O. Fayet, and C. Georgopoulos. 1991. The universally conserved GroE (Hsp60) chaperonins. *Annu. Rev. Microbiol.* 45: 301–325.